Volume 3, Issue 6, 2025

Frontier in Medical & Health Research

ISSN: (e) 3007-1607 (p) 3007-1593

MOLECULAR DOCKING STUDY OF QUINOLIN-4(1H)-ONE DERIVATIVES AS VEGFR-2 INHIBITORS FOR THE TREATMENT OF LUNG CANCER

Sunbal Khan[1], Ihsan Ullah[2], Adnan Shahzad[*3], Muhammad Omer[4], Imad Ud Din[5], Farhat Iqbal[6], Husna Iqbal[7], Asad Ullah Khan[8], Sumeera[9], Sidratul Muntaha[10], Kausar[11], Nadia Subhan[12]

[1,2 *3,4,5,6,7,8,9,11]*Institute of Chemical Sciences, University of Swat, Swat, Pakistan*

[10,12]*Center for Plant Science and Biodiversity, University of Swat, Swat, Peshawar Medical College, Peshawar, KP, Pakistan*

[2]ihsanmtk@uswat.edu.pk, [*3]adnanshahzad@uswat.edu.pk

DOI: https://doi.org/10.5281/zenodo.16720148

Keywords
VEGFR-2, lung cancer, quinolin-4(H)-one derivatives, virtual screening

Article History
Received: 28 May, 2025
Accepted: 15 July, 2025
Published: 01 August, 2025

Corresponding Author: *
Adnan Shahzad

Abstract

A tyrosine kinase receptor (TKR), vascular endothelial growth factor receptor-2 (VEGFR-2), is often overexpressed in the majority of tumors. It is essential for tumor angiogenesis because it mediates important angiogenic biological signals, such as vascular permeability, endothelial cell survival, migration and proliferation. VEGFR-2 has become an acceptable therapeutic target against cancer because of its critical role in facilitating tumor vasculature. Inhibiting the VEGF signaling pathways has emerged as a useful cancer therapeutic strategy. This study designed and developed a variety of quinolin-4(1H)-one derivatives that are strong inhibitors of VEGFR-2 (KDR) kinase. These substances were developed with a urea moiety and quinoline scaffold, and their biological activity against VEGFR-2 was examined. The compound with the most inhibitory action on VEGFR-2 was Q2. The preliminary pharmacophoric hypothesis was validated by docking data, which also indicated a common mechanism of interaction at the ATP-binding site of VEGFR-2. This suggests that substance Q2 is a promising cancer therapeutic drug that deserves further research.

The Quinolone scaffold was initially discovered to have antimicrobial properties, and its derivatives were found to have a variety of pharmacological activity, such as anticancer properties. Derivatives of quinolin-4(H)-one have been found to block a number of proteins and enzymes, including phosphoinositide 3-kinases (PI3K), that are implicated in the proliferation of cancer cells. Quinolones have also been investigated as EGFR and VEGFR protein kinase inhibitor.

Using auto dock vina, discovery studio, and PyMol, we examined the molecular interactions of 10 bioactive compounds against VEGFR-2 in present work. In the docking test, the chosen quinolin-4(H)-one derivatives showed good inhibitory action with target proteins. The binding interactions' affinities range from -14.65 to -11.31 Kcal/mol, and the chosen hits' docking result is similar to that of regular sorafenib. Of all the compounds that were examined, Q2 had the highest docking score, Q6 the lowest binding interaction against VEGFR-2.

INTRODUCTION

The lung is a specially designed organ with a large surface exposed to dangerous substances directly in the environment due to its distinctive shape. An excessive amount of reactive oxygen species (ROS)

Frontier in Medical & Health Research

ISSN: (e) 3007-1607 (p) 3007-1593

are produced when people continuously breathe in car exhaust, cigarette smoke, and infectious virus particles in contaminated air, which cause inflammatory reactions, resistance to apoptosis, and other factors that greatly aid in the start of carcinogenesis [1, 2]. With a high rate of morbidity and death, lung carcinoma is a dangerous tumor that develops from the lung glands. [3]. According to GLOBOCAN and the International Agency for Research on Cancer (IARC) 2020, lung cancer is the second most frequent cancer globally, with breast cancer at the top. According to a 2018–2020 study conducted at Shifa International Hospital, adenocarcinomas accounted for 38% of all instances of lung cancer, with many of these cases manifesting at advanced stages. [4]. Globally, lung cancer is the greatest prevalent cancer and primary cause of cancer-related fatalities. About 1.8 million deaths every year, according to estimates of all lung cancers, 80–85% are non-small cell lung cancers (NSCLCs) [5-9].

The primary feature of cancer is the uncontrolled development of cells that need nutrients and oxygen from the blood supply.Angiogenesis, a procedure that uses existing blood vessels to generate new ones, satisfies this requirement. EGF (epidermal growth factor), VEGF (vascular endothelial growth factor), FGF (fibroblast growth factor), PDGF (platelet derived growth factor), and TGF-α (transforming growth factor alpha), are among the growth factors that strictly regulate angiogenesis under normal physiological situations [10, 11]. Neovascularization is essential for proliferation and for cancer cell spreading of; the most significant of these neovascularization paths is VEGF-A/VEGFR-2 signaling pathways [12, 13]. The way that VEGF reacts to particular receptors determines its biological action. VEGFR2, which is thought to be the primary VEGF signal sensor in ECs, activates directly adhesion and PI3K/Akt signal pathways by triggering adhesion kinase (FAK) [14]. VEGFRs can be targeted and inhibited by blocking their molecules and receptors in order to treat VEGF/VEGFR-associated disorders [15]. Angiogenesis inhibitors appear to work best when combined with other treatments for a variety of cancers because of their capacity to prevent and delay tumor growth [16, 17]. VEGF functions through tyrosine kinase receptors, including VEGFR-1, VEGFR-2, and VEGFR-3. A potential strategy for treating cancer is to target the VEGF/VEGFR-2 pathway. Sunitinib, sorafenib, lenvatinib and vandetanib, are the four medications that entail VEGFR-2 inhibition, illustrating the proven advantages of VEGFR-2 inhibitors [18-21].

Quinoline, a heterocyclic aromatic compound have reportedly been employed as anticancer medicines to treat different kinds of cancer. With an IC50 of 1.58 to 157 μM, the quinoline derivative demonstrated a cytotoxic impact and suppressed the growth of NCI-H226 lung cancer cells. Because these compounds solely target cancer cells and do not affect healthy cells, this condition shown that they can be active agents against lung tumor [22]. Quinolin-4(1H)-one derivatives are a versatile class of alkaloid in organic chemistry that are known to have activity against Plasmodium spp., the parasite that causes malaria. These compounds also display other biological activities, including, antiproliferative [23], antitumor [24], antifungal [25], cytotoxic [26], antimycobacteril [27], antioxidant [28], anti-allergic asthma [29], anticancer [30], insecticidal [31] properties.

Investigation on novel small chemical compounds containing quinolin-4(1H)-one scaffolds for their ability to inhibit VEGFR-2 was motivated by preliminary studies on the anti-tumor properties of quinolin-4(1H)-one derivatives. Sorafenib, a standard lung cancer inhibitor, and derivatives of quinolin-4(1H)-one were used in a recent work to demonstrate the binding conformation and mechanism of VEGFR-2 using molecular docking analysis.

1. Methodology

2.1 Molecular Docking

The mechanism of the binding contact of proposed quinolin-4(1H)-one compounds was investigated for competitive and non-competitive suppression of lung cancer enzymes, VEGFR-2 (KDR/Flk-1) [32] the molecular docking procedure. The three dimensional crystal structures of protein was taken from the Protein Databank and designed quinolin-4(1H)-one and standard sorafenib are given in **figure 1**. Initially, Auto Dock and MGL technologies were used to theoretically prepare the title proteins [33]. For ease of calculation, inhibitors, co-factors, heteroatoms, and all water molecules were eliminated for optimization [34]. The docking

Volume 3, Issue 6, 2025

Frontier in Medical & Health Research

ISSN: (e) 3007-1607 (p) 3007-1593

conformer with the lowest binding energy and the highest stability was selected for further investigation. Discovery Studio Visualization, PyMol, and Auto Dock Vina [35], and other software were utilized to display images of proteins-ligand complexes, their mechanisms, and the docking positions of particular Quinolin-4(1H)-one derivatives against target enzymes

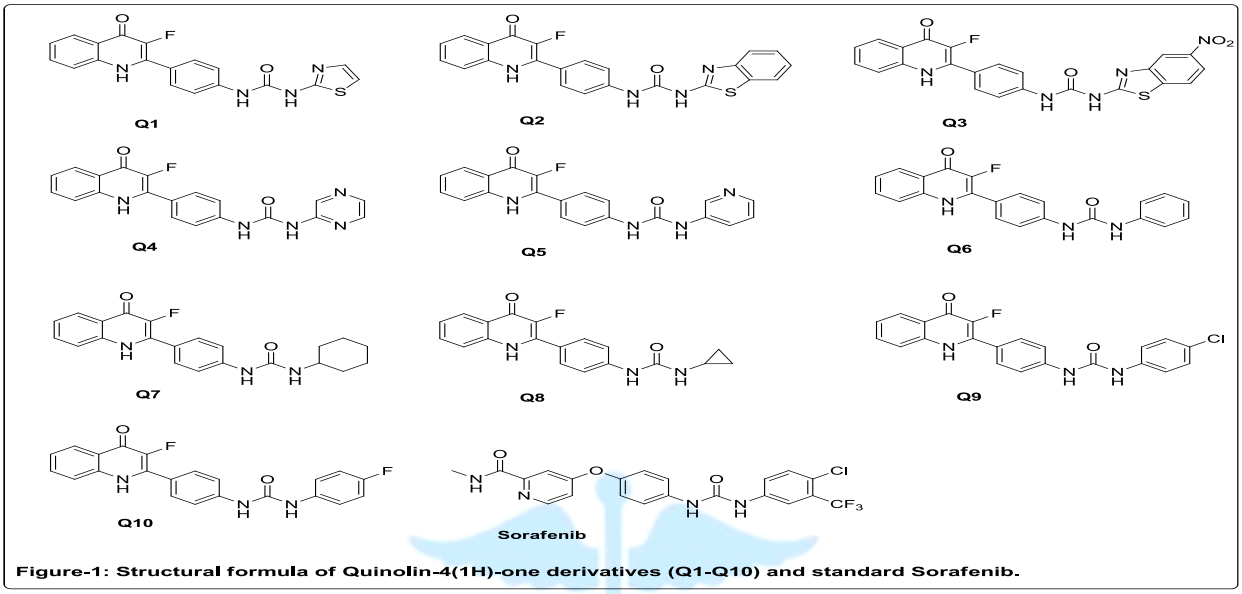

Figure-1: Structural formula of Quinolin-4(1H)-one derivatives (Q1-Q10) and standard Sorafenib.

2.2 Design strategy

According to published pharmacophore modeling and virtual screening study, the majority of VEGFR-2 inhibitors have four crucial pharmacophoric features. The traits include:

(a) A flat heteroaromatic ring with a hydrogen bond acceptor core that forms hydrogen bonds with the NH group of crucial Cys919 (and in some cases Glu917 were also binds by H-bond) in the ATP binding domain (hinge region). (b) A core aromatic system located in the linker area. (c) The DFG domain is occupied by a hydrogen bond donor and acceptor moiety (HBAHBD), it may be a urea or amide group and it connects with ASP-1046 and GLU-885 in the enzyme DFG motif. At this region two H-bonds are formed CO group of amide or urea and ASP-1046 and another H-bond between NH of amide or urea and GLU-885. (d) A hydrophobic tail at the end that is positioned inside the hydrophobic allosteric pocket **(Figure 2)** [36-39].

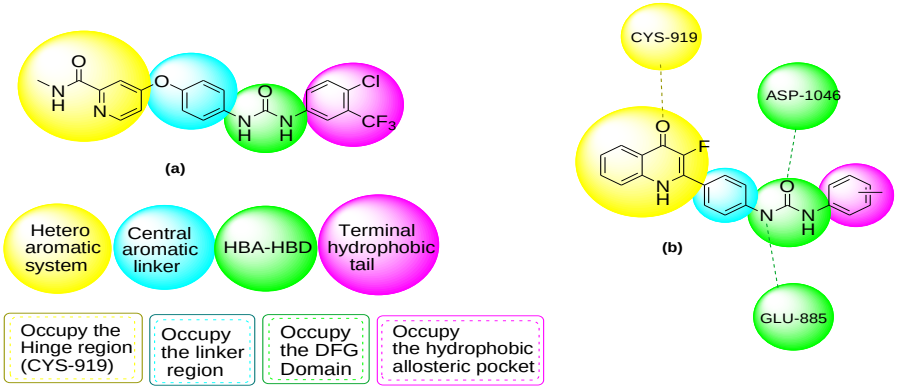

Figure-2: The essential pharmacophoric features of VEGFR-2 inhibitorsapplied to Sorafenib (a) and Quinolin-4(1H)-one derivatives (b).

Frontier in Medical & Health Research

ISSN: (e) 3007-1607 (p) 3007-1593

3. Results and Discussion

3.1 Molecular docking analysis of specific compounds

Molecular docking modeling was utilized to examine binding mechanism of active drugs **(Q1-Q10)** within the active site of VEGFR-2 in contrast to Sorafenib.

Interaction between Q1 and VEGFR-2: The docking results of compound **Q1** against VEGFR2 showed binding energies of -11.62 kcal/mol and an inhibition constant of 3.01 nM (nanomolar), as shown in **Table 1** [40, 41] **.**The compound **Q1** bounded well with VEGFR-2 active site. Compound Q1 showed interactions with the residue CYS-919, GLU-885, ASP-1046, GLU-917, VAL-916, LEU-840, LEU-889, LEU-1035, VAL-889, VAL-848 and ALA-866 of VEGFR-2 active site. The urea (HBA-HBD) and heteroaromatic region of compound Q1 form H-bonds with the residue CYS-919 (O...NH, 1.6 Å), GLU-885 (NH....O, 2.2 Å) and ASP-1046 (O....HN, 2.2 Å) of enzyme as show in **table 2 [37].** The said compound also incorporated in π-alkyl, π -sigma and weak Vander Waal interactions with GLU-917, VAL-916, LEU-840, LEU-889, LEU-1035, VAL-889, VAL-848 and ALA-866 [39]residues of Q1 compound given in **figure 3(E).**

Interaction between Q2 and VEGFR-2: The best inhibition against VEGFR-2 was demonstrated by the docking pose of the chosen drug **Q2**, which had binding energies of -14.65 kcal/mol and an inhibition constant of 18.28 pM (picomolar), as shown in **table 1** [40]. The chosen chemical Q2 was permitted to dock deep within the center core formed by VEGFR-2's active residues. The mentioned chemical Q2's mechanism of interaction with the VEGFR-2 enzyme revealed interactions with CYS-919, GLU-885, ASP-1046, GLU-917, PHE-918, LEU-840, LEU-840, VAL-916, PHE-1047, VAL-884, VAL-899,AL-866, LEU-1035,LEU-1019 and CYS-1045 of VEGFR-2 active site. The oxygen and fluorine atom of flat heteroaromatic ring form hydrogen bond with CYS-919 (O...NH, 1.7 Å) [37], so the residue CYS-919 is strongly bounded to the flat heteroaromatic region of selected ligand by two hydrogen bonds. The NH-group of urea region of the ligand make hydrogen bond with GLU-885 (NH....O, 2.2 Å). The nitrogen and oxygen atoms of urea region (HBA-HBD) make also H-bonds with ASP-1046 (O....NH, 1.8 Å) residues [37]. Compound Q2 make weak Vander Waal, π-sigma and π-alkyl interactions with GLU-917, PHE-918, LEU-840, LEU-840, VAL-916, PHE-1047, VAL-884, VAL-899,AL-866, LEU-1035,LEU-1019 AND CYS-1045 [39] amino acids. Additionally, the selected ligand Q2 also incorporated in π-π stacking with CYS-919 (O....O, 2.9 Å) and ASP-1046 (O.....O, 2.7 Å) residues of VEGFR-2 portrayed in **figure 4(E)**.

Interaction between Q3 and VEGFR-2: Based on the docking parameter, the title **Q3** molecule was found to interact with VEGFR-2 with an inhibition constant of 1.06 nM (nanomolar) and a binding energy value of -12.24 kcal/mol [36], given in **Table 1**. Within the VEGFR-2 active cavity, the molecule Q3 was predicted to create a crucial interaction with CYS-919, LYS-868, ASP-1046, GLU-917, PHE-918, LEU-899, LEU-840, LEU-1035, VAL-916, VAL-848, ALA-866 and CYS-1045 of VEGFR-2 active residues of enzyme [37, 39]. Among these interactions, the said ligand forms three hydrogen bonds with enzyme. It makes one H-bond with CYS-919 (O...NH, 1.8 Å) at hinge region with oxygen atom of the ligand, and two H-bonds with LYS-868 (O...NH, 1.9 Å) and ASP-1046 (O...NH, 1.9 Å) at the DFG-Domain region (HBA and HBD region) [37]. expressed in **table 2** [40]. GLU-917 and PHE-918 interact with fluorine atom at the hinge region. LEU-840 and LEU-889 make π-sigma interactions with compound. The residue CYS-1045 interact via π-sulfur bonding with ligand in the active site. Other amino acids bind via π-alkyl interactions with the Q3. The GLU-917 and PHE-918 make bonds with fluorine atom of flat aromatic region (hinge region). Moreover, the said compound **Q3** also make π-alkyl bonds with VAL-848, VAL-916, LEU-1035 and ALA-866. CYS-1045 residue interact by π-sulfur interactions. It also make π- π stacking interactions with CYS-919 (O...O, 2.8 Å), ASP-1046 (O...O, 2.5 Å) and GLU-885 (O...O, 3.1 Å) [37], shown in **figure 5(E)**.

Interaction between Q4 and VEGFR-2: Based on the docking parameter, it was found that the title chemical **Q4** bound to VEGFR-2 with an inhibition constant of 229.29 pM (picomolar), as shown in **Table 1**, and a binding energy value of -13.15

Frontier in Medical & Health Research

ISSN: (e) 3007-1607 (p) 3007-1593

kcal/mol [40]. Within the VEGFR-2 active cavity, the molecule Q4 was predicted to create a crucial contact with CYS-919, GLU-885, ASP-1046, GLU-917, VAL-916, LEU-840, LEU-1035, LEU-899, PHE-1047, VAL-848, VAL-899, ALA-866, and CYS-1045 of VEGFR-2 active active residues of enzyme [37, 39]. These interactions include the formation of three hydrogen bonds between the ligand and the enzyme. It make one H-bond with CYS-919 (O….NH, 1.7 Å) at hinge region, and two H-bonds with GLU-885 (NH….O, 2.1 Å) and ASP-1046 (O….NH, 1.7 Å) at the DFG-Domain region (HBA and HBD region) [37], represented in **Table 2**. The said compound **Q4** also form weak Vander Waal, π-alkyl, π-sigma and alkyl bonds with GLU-917, VAL-916, LEU-840, LEU-1035, LEU-899, PHE-1047, VAL-848, VAL-899, ALA-866, and CYS-1045 active residues of VEGFR-2. Moreover, the ASP-1046 (O…..O, 2.4 Å) also form π- π stacking with the selected ligand, expressed in **figure 6(E)**.

Interaction between Q5 and VEGFR-2: According to **Table 1**, the binding positions of candidate ligand **Q5** demonstrated good inhibition against VEGFR-2 with binding energy value of -12.71 kcal/mol [40] and an inhibition constant of 484.75 pM (picomolar). According to the docking analysis, hit compound Q5 has a high probability of bonding with the target protein and becoming highly stable inside the active pocket of the enzyme.The said ligand form three hydrogen bonds with enzyme. It make one H-bond with CYS-919 (O….HN, 1.8 Å) at hing region, and two H-bonds with GLU-885 (NH….O, 2.0 Å) and LYS-868 (O….NH, 1.8 Å) at the DFG-Domain region (HBA and HBD region) [37], demonstrated in **Table 2**. In addition, the residue VAL-916, LEU-840 AND LEU-889 make π-sigma bonds with Q4. Weak Vander Waal and π-alkyl interactions with LEU-1035, ALA-866, VAL-848, VAL-899 and CYS-1045 amino acids further stabilizes the complex. Besides, the CYS-919 (O….O, 3.2 Å) and GLU-885 (O….O, 3.2 Å) make π-π stacking with the receptor shown in **figure 7(E)**[37, 39, 42].

Interaction between Q6 and VEGFR-2: The title ligand **Q6** was shown to bind with VEGFR-2 based on the docking parameter, with a binding energy value of -11.31 kcal/mol [40] and an inhibition constant of 5.10 nM (nanomolar), as shown in **Table 1**. Within the VEGFR-2 active cavity, the molecule Q6 was predicted to create a crucial contact with ASP-1046, CYS-919, GLY-922, CYS-1045, VAL-916, LEU-1035, LEU-840, VAL-899, VAL-914, VAL-848, and LYS-868 active residues of enzyme [37]. Among these interactions, the selected ligand form three hydrogen bonds with residue ASP-1046 (O….NH, 2.2 Å), CYS-919 (NH…O, 2.3 Å) and GLY-922 (O….HN, 2.6 Å) [37] represented in **Table 2**. Further, **Q6** compound also make weak Vander Waal, π –sigma, π-alkyl and alkyl bonds with CYS-1045, VAL-916, LEU-1035, LEU-840, VAL-899, VAL-914, VAL-848, and LYS-868 active residues of VEGFR-2 expressed in **figure 8(E)**. Additionally, the CYS-919 (O…O, 2.5 Å) and ASP-1046 (O….O, 2.9 Å) make π-π stacking with the receptor, expressed in **figure 8(E)**.

Interaction between Q7 and VEGFR-2: The title ligand **Q7** was shown to bind with VEGFR-2 with an inhibition constant of 79.41 pM (picomolar) based on the docking parameter, and binding energy value of -13.78 kcal/mol [40] and given in **Table 1.** The chemical Q7 was predicted to be present in the VEGFR-2 active cavity and established a crucial contact with CYS-919, GLU-885, ASP-1046, GLU-917, PHE-918, PHE-1047, VAL-899, VAL-916, LEU-840, LEU-1035 and CYS-1045 [39] of VEGFR-2 active active residues of enzyme [37]. Among these interactions, the said ligand forms three hydrogen bonds with enzyme. It makes one H-bond with CYS-919 (O….HN, 1.9 Å) at hinge region with oxygen atom, and two H-bonds with GLU-885 (NH….O, 2.3 Å) and ASP-1046 (NH….O, 1.8 Å) at the DFG-Domain region (HBA and HBD region) [37], represented in **Table 2**. It also form π-π T-shaped interactions with PHE-918 and PHE-1047 amino acids. The GLU-917 make bond with fluorine atom of flat aromatic region (hinge region). Moreover, the said compound **Q7** also make π-alkyl bonds with VAL-899, VAL-916, LEU-840, LEU-1035 and CYS-1045 active amino acids of VEGFR-2 expressed in **figure 9(E)**.

Interaction between Q8 and VEGFR-2: Using molecular docking, the method by which **Q8** binds

Frontier in Medical & Health Research

ISSN: (e) 3007-1607 (p) 3007-1593

to the VEGFR-2 active site and its inhibitory effect were examined, expressed in **Table 1.** The native ligand had a 1.26 nM (nanomolar) inhibition constant and an affinity score of -12.02 kcal/mol [36]. The **Q8** fully filled the cavity and was buried deep within the VEGFR-2 active site. It established H-bonds with crucial residues CYS-919 (O...HN, 2.6 Å), GLU-885 (NH....O, 2.2 Å), and ASP-1046 (O....HN, 1.9 Å) of receptor [37]. The finest position of Q8 revealed the development of three hydrogen bonds with the CYS-919 with oxygen of ATP-binding region (Hinge region), GLU-885 and ASP-1046 DFG-Domain or HBA-HBD region (urea group of selected ligand) depicted in [37] **table 2**. The GLU-917 make bond with fluorine atom of flat aromatic region (hinge region). The residue VAL-916 and LEU-840 make π-sigma interactions with the flat aromatic region and linker region. Additionally, VAL-899, VAL-848, CYS-1045, LEU-1035, ALA-866 [39] bounded with ligand via π-alkyl bonds **figure 10(E)**.

Interaction between Q9 and VEGFR-2: To determine the inhibitory action of the stated ligand **Q9** against VEGFR-2, the docking setup was evaluated. The mentioned chemical Q9 had a high affinity value of -11.58 kcal/mol and was completely fitted within the VEGFR-2 active site [40] and an inhibition constant of 3.26 nM (nanomolar) given in **Table 1**. It was expected that compound Q9 would significantly reduce VEGFR-2 activity and form a crucial interaction with the receptor's active residues, which are what give it its inhibitory effect. The oxygen atom of hinge region bound with ASP-1046 (O....HN, 2.3 Å) by hydrogen bond and act as hydrogen bond acceptor. The oxygen motif of HBA-HBD region involved in H-bonding with CYS-919 (O...NH, 2.4 Å) and GLY-922 (O...HN, 2.8 Å) [37] demonstrated in **Table 2**. The residue LYS-868 make π-cation interactions with the hinge region of selected ligand. Additionally, weak Vander Waal forces, π-sigma and π-alkyl interactions were found between the target ligand and active residues VAL-848, VAL-916, LEU-840, LEU-1035, ALA-866, VAL-914 of enzyme VEGFR-2 shown in **figure 11(E)**.

Interaction between Q10 and VEGFR-2: Using molecular docking, the method by which **Q10** binds to the VEGFR-2 active site and its inhibitory effect were examined. **Table 1** indicates that the native ligand had an affinity score of -13.50 kcal/mol [40] and an inhibition constant of 127.10 pM (picomolar). The compound **Q10** was entirely buried within the VEGFR-2 active site and filled its cavity. It demonstrated important H-bonds interactions with key amino acids CYS-919 (O....HN, 1.7Å), GLU-885 (NH....O, 2.2 Å) and LYS-868 (O....HN, 2.4 Å) of receptor [37, 39]. The best pose of compound demonstrated the formation of three hydrogen bonds, the CYS-919 with oxygen of ATP-binding region (Hinge region), GLU-885 and LYS-868 DFG-Domain or HBA-HBD region (urea group of selected ligand) depicted in [37] **table 2.** The GLU-917 and PHE-918 make bond with fluorine atom of flat aromatic region (hinge region). The residue VAL-916 LEU-889 and LEU-840 make π-sigma interactions with ligand. VAL-899, VAL-848, CYS-1045, LEU-1035, ALA-866 bounded with ligand via π-alkyl bonds. Moreover, CYS-919 (O....O, 3.0 Å) make π- π stacking with ligand **figure 12(E)**

Table 1. Binding energies in (kcal/mol) and inhibition constant of compounds Q1-Q10 and Sorafenib with VEGFR-2

Compounds	Binding Energy (kcal/mol)	Inhibition Constant of
Q1	-11.62	3.01 nM
Q2	-14.65	18.28 pM
Q3	-12.24	1.06 nM
Q4	-13.15	229.29 pM
Q5	-12.71	484.75 pM
Q6	-11.31	5.10 nM
Q7	-13.78	79.41 pM

Frontier in Medical & Health Research

ISSN: (e) 3007-1607 (p) 3007-1593

Q8	-12.02	1.26 nM
Q9	-11.58	3.26 nM
Q10	-13.50	127.10 pM
Sorafenib	-15.19	3.33 pM

. **Table 2.** Residues involved in interactions and their distances of selected compounds with VEGFR-2

Compounds	Interacting amino acids	Interactions	Types of interactions	Distances(Å)
Q1	CYS-919, GLU-885, ASP-1046	O...HN, NH...O, O...NH	H-Bonding	1.6, 2.2, 2.2
Q2	CYS-919, GLU-885, ASP-1046	O...HN, NH...O, O...NH	H-Bonding	1.7, 2.2, 1.8
	CYS-919, ASP-1046	O...O, O...O	π-π interaction	2.9, 2.7
Q3	CYS-919, ASP-1046, LYS-868	O...HN, O...HN, O...HN	H-Bonding	1.8, 1.9, 2.2
	CYS-919, ASP-1046	O...O, O...O	π-π interaction	2.8, 2.5
Q4	CYS-919, GLU-885, ASP-1046	O...HN, NH...O, O...NH	H-Bonding	1.7, 2.1, 1.7
	ASP-1046	O...O	π-π interaction	2.4
Q5	CYS-919, GLU-885, LYS-868	O...HN, NH...O, O...HN	H-Bonding	1.8, 2.0, 1.8
	CYS-919, GLU-885	O...O, O...O	π-π interaction	3.2, 3.2
Q6	CYS-919, GLY-922, ASP-1046	NH...O, O...HN, O...HN	H-Bonding	2.3, 2.6, 2.2
	Asp-1046	O...O	π-π interaction	2.5, 2.9
Q7	CYS-919, GLU-885, ASP-1046	O...HN, NH...O, O...HN	H-Bonding,	1.9, 2.3, 1.8
Q8	CYS-919, GLU-885, ASP-1046	O...HN, NH...O, O...HN	H-Bonding	2.6, 2.2, 1.9
Q9	CYS-919, GLY-922, ASP-1046	O...HN, O...HN, O...HN	H-Bonding	2.4, 2.8, 2.3
Q10	CYS-919, GLU-885, LYS-868	O...HN,NH..O, O..HN	H-Bonding	1.7, 2.2, 2.4
	CYS-919	O...O	π-π interaction	3.0

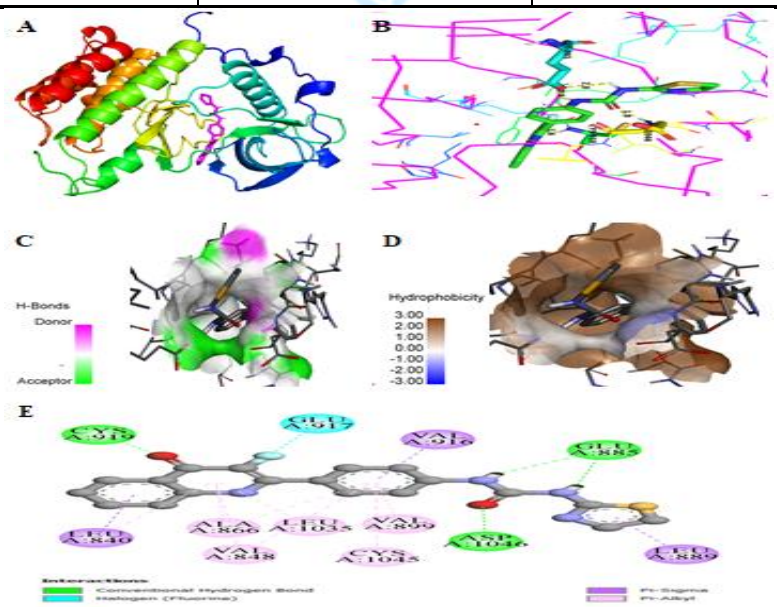

Figure-3: Binding poses of Q1 with VEGFR-2, (A) complex, (B) 3D interactions, (C) H-bonding, (D) hydrophobic bonding, and (E) 2Dinteractions.

Frontier in Medical & Health Research

ISSN: (e) 3007-1607 (p) 3007-1593

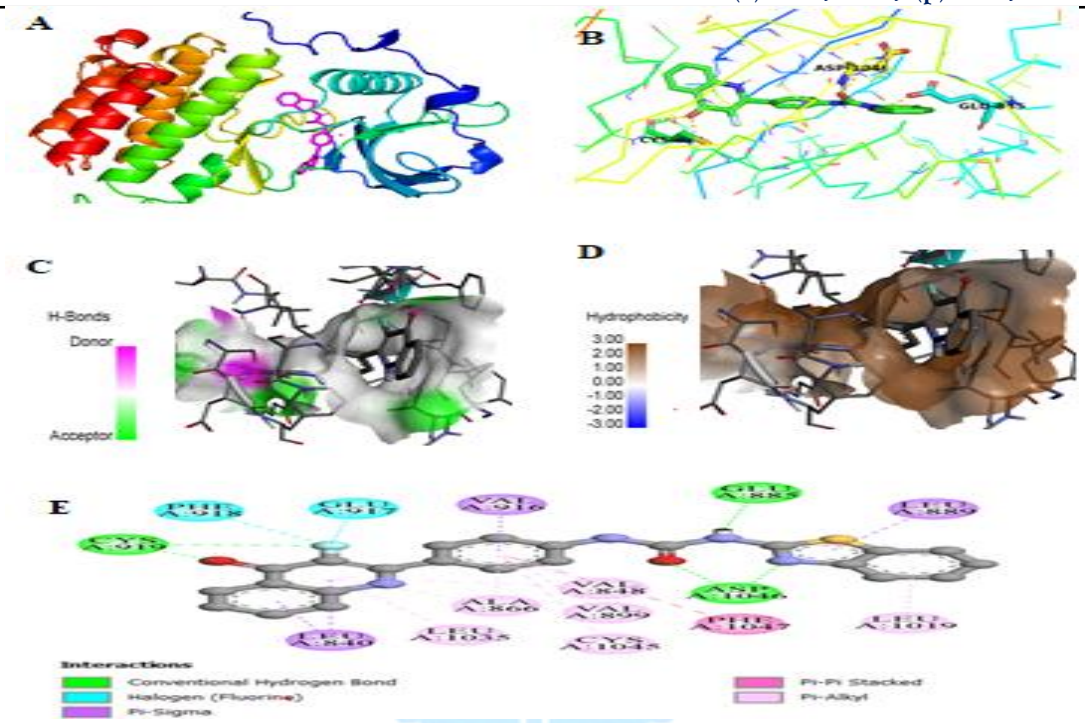

Figure-4: Binding poses of Q2 with VEGFR-2, (A) complex, (B) 3D interactions, (C) H-bonding, (D) hydrophobic bonding, and (E) 2Dinteractions.

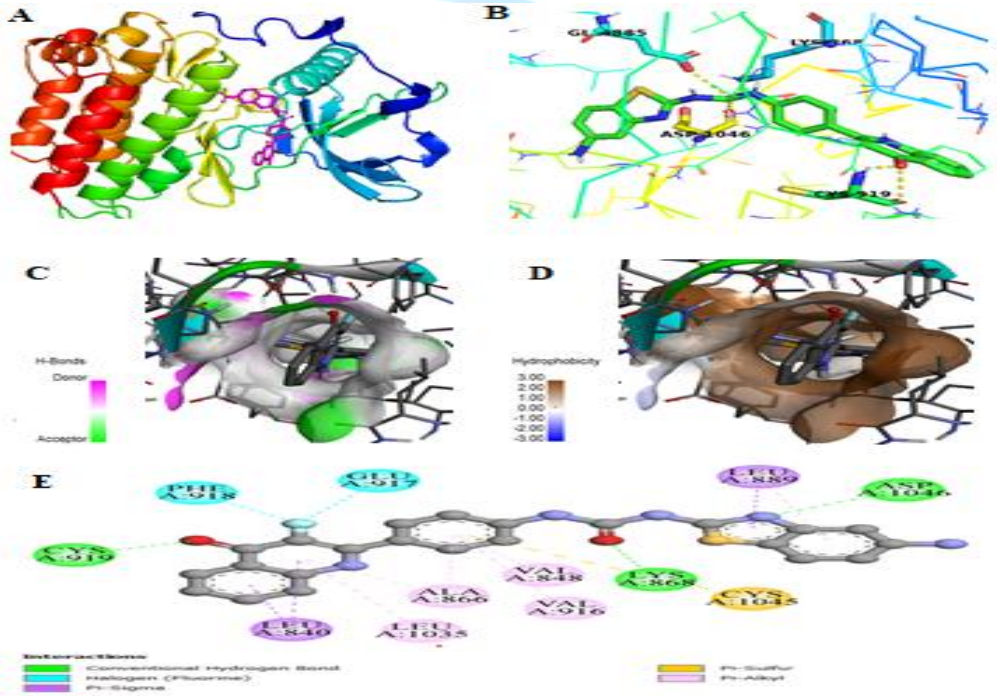

Figure-5: Binding poses of Q3 with VEGFR-2, (A) complex, (B) 3D interactions, (C) H-bonding, (D) hydrophobic bonding, and (E) 2Dinteractions.

Frontier in Medical & Health Research

ISSN: (e) 3007-1607 (p) 3007-1593

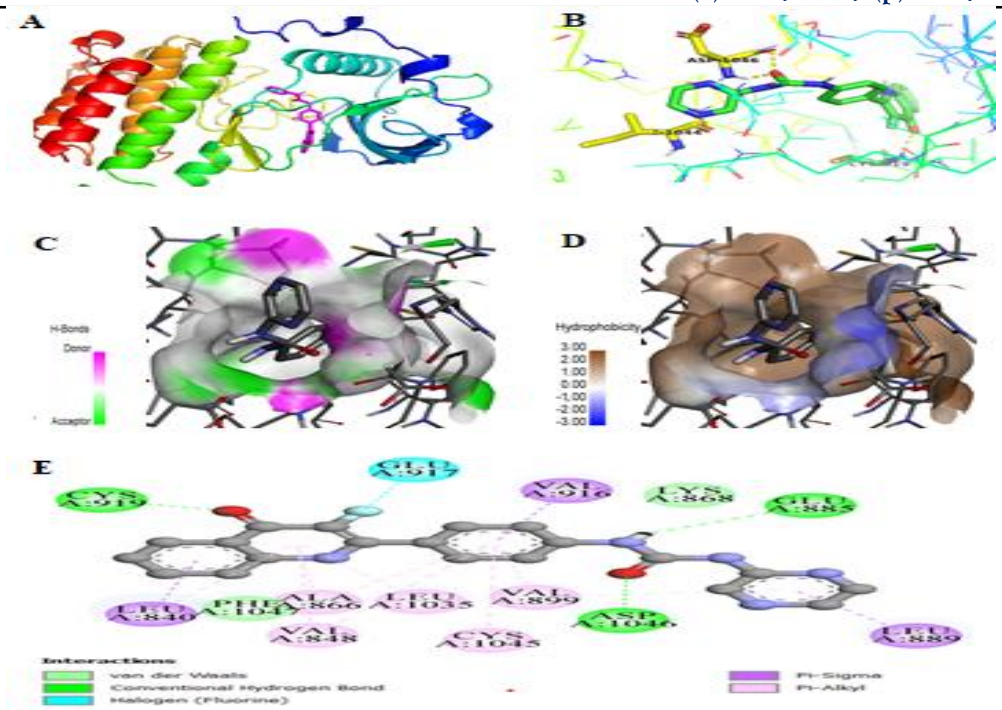

Figure-6: Binding poses of Q4 with VEGFR-2, (A) complex, (B) 3D interactions, (C) H-bonding, (D) hydrophobic bonding, and (E) 2Dinteractions

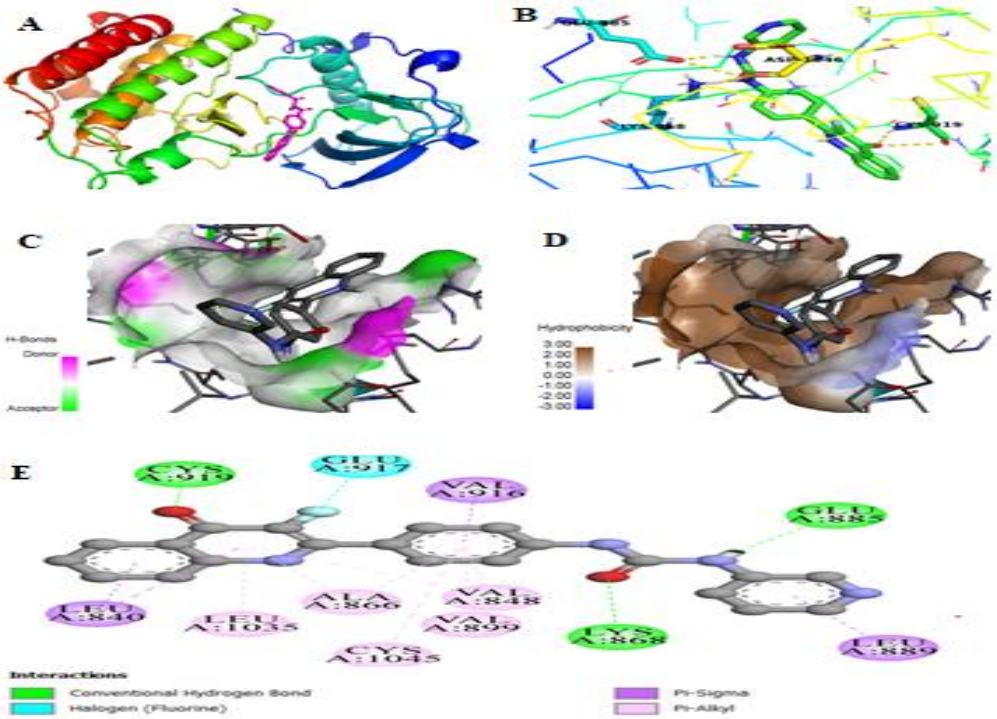

Figure-7: Binding poses of Q5 with VEGFR-2, (A) complex, (B) 3D interactions, (C) H-bonding, (D) hydrophobic bonding, and (E) 2Dinteractions

Frontier in Medical & Health Research

ISSN: (e) 3007-1607 (p) 3007-1593

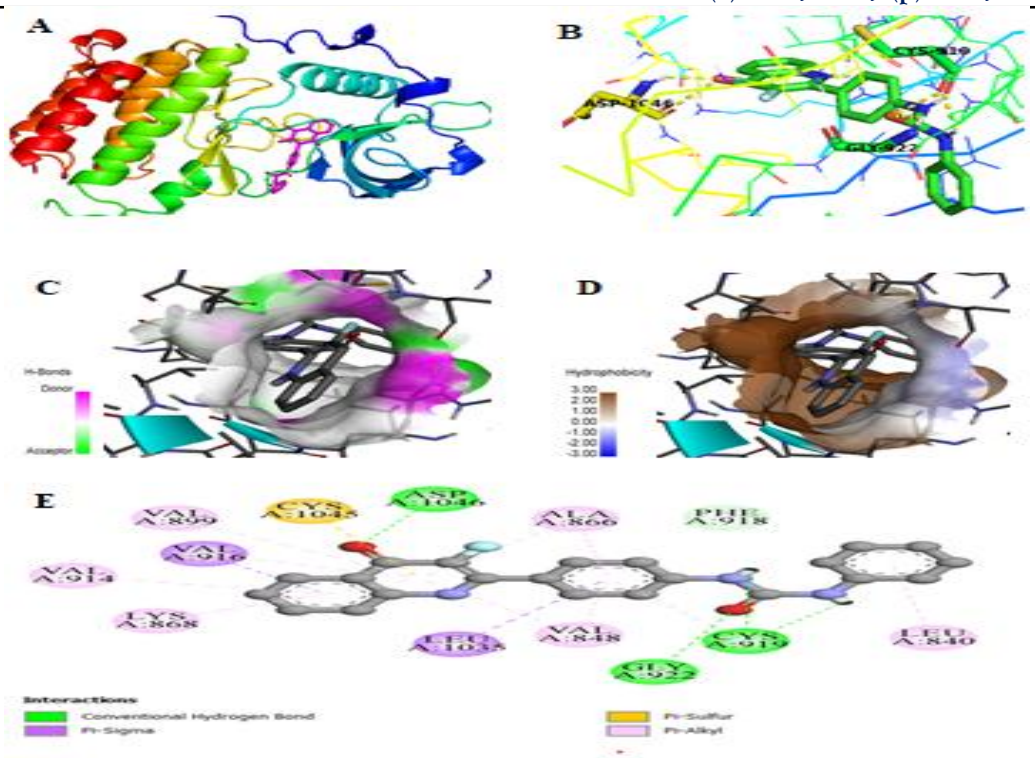

Figure-8: Binding poses of Q6 with VEGFR-2, (A) complex, (B) 3D interactions, (C) H-bonding, (D) hydrophobic bonding, and (E) 2Dinteractions

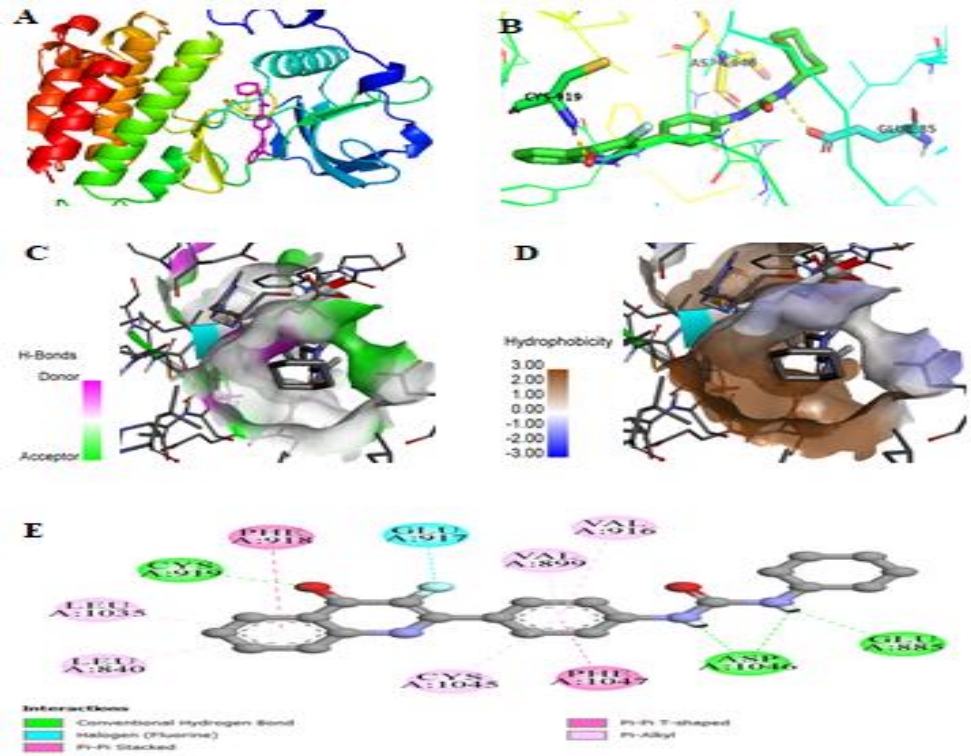

Figure-9: Binding poses of Q7 with VEGFR-2, (A) complex, (B) 3D interactions, (C) H-bonding, (D) hydrophobic bonding, and (E) 2Dinteractions

Frontier in Medical & Health Research

ISSN: (e) 3007-1607 (p) 3007-1593

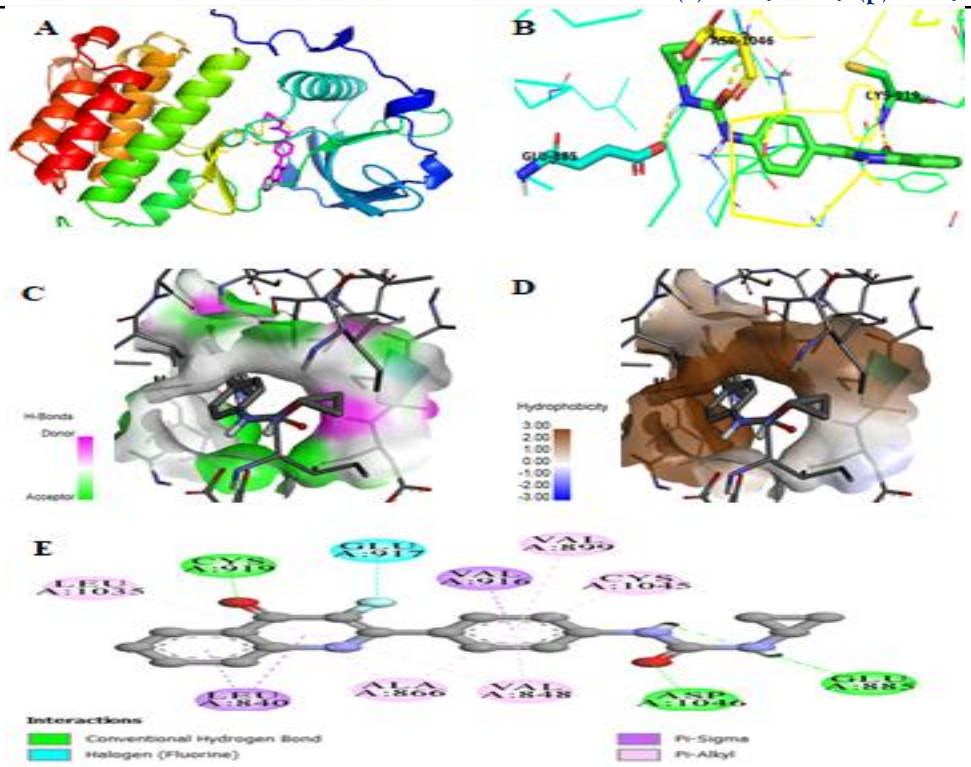

Figure-10: Binding poses of Q8 with VEGFR-2, (A) complex, (B) 3D interactions, (C) H-bonding, (D) hydrophobic bonding, and (E) 2Dinteractions

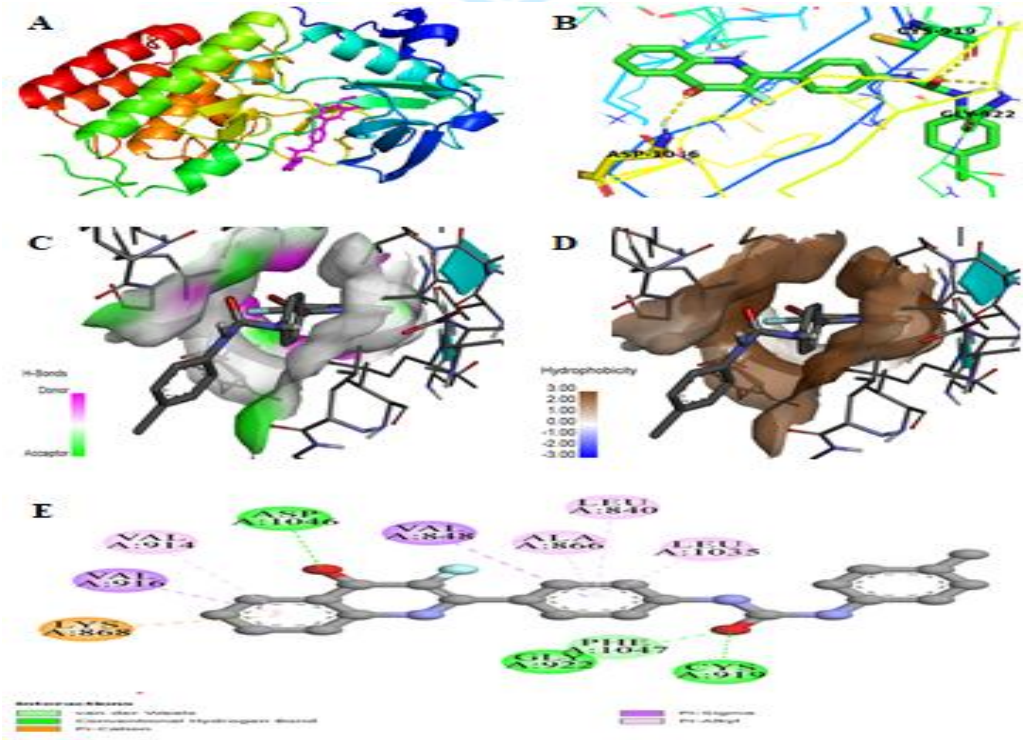

Figure-11: Binding poses of Q9 with VEGFR-2, (A) complex, (B) 3D interactions, (C) H-bonding, (D) hydrophobic bonding, and (E) 2Dinteractions

Frontier in Medical & Health Research

ISSN: (e) 3007-1607 (p) 3007-1593

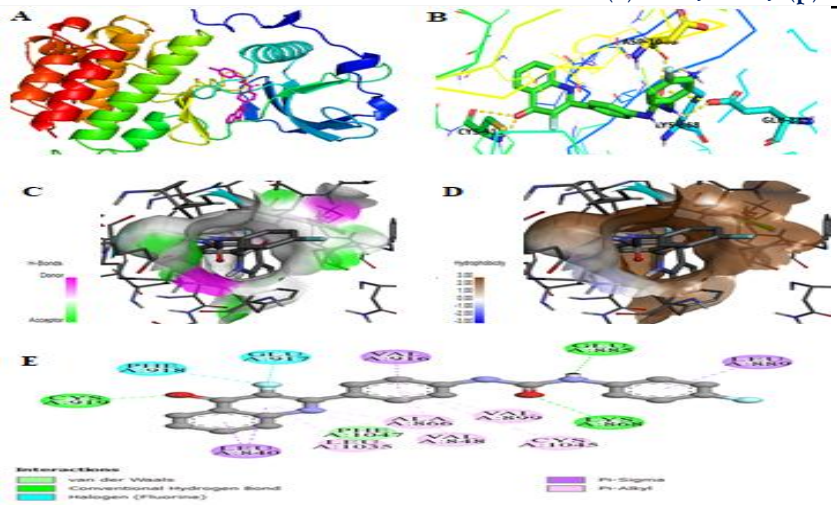

Figure-12: Binding poses of Q10 with VEGFR-2, (A) complex, (B) 3D interactions, (C) H-bonding, (D) hydrophobic bonding, and (E) 2Dinteractions

4. Conclusion

In conclusion, Quinolin-4(1H)-one is a crucial scaffold in the field of drug development because of its strong anticancer properties and distinct mode of action. It has become more well-known in recent years and is the basis for a wide range of pharmacological products. Its importance has been emphasized by the convincing outcomes seen in many research, particularly when it comes to cancer treatment. Numerous Quinolin-4(1H)-one compounds have already entered clinical trials. Quinolin-4(1H)-one derivatives have become intriguing options in the hunt for novel anticancer medications because of their diverse chemical structures and biological action. This article shows the inhibition action of Quinolin-4(1H)-one derivatives on VEGFR-2 for treatment of lung cancer.

Docking against the PDB-derived crystal structure of VEGFR-2 was done, and the target proteins' binding interactions and docking scores with the chosen variants were analyzed [43].The screening compounds that were selected showed a similar docking score to the control inhibitors that were used [44]. The results of the docking studies demonstrated that the drugs examined, which ranged from Q1 to Q10 (-11.31-14.65 kcal/mol), exhibited good inhibitory efficacy against VEGFR-2 (shown in Table 1), comparative to Sorafenib (-15.19 kcal/mol). Overall results shows that Q2 is most active and Q6 is least active inhibitor among all ten selected ligands against VEGFR-2. These compounds were developed as type-II inhibitors after a thorough SAR analysis [45]. According to these results, quinolin-4(1H)-one derivatives may be a strong candidate to be taken into account while creating new, potent VEGFR-2 inhibitors.

References

Zhang, J., et al., The role of cGAS-STING signaling in pulmonary fibrosis and its therapeutic potential. Frontiers in Immunology, 2023. **14**: p. 1273248.

Hou, Y., et al., Dissecting the pleiotropic roles of reactive oxygen species (ROS) in lung cancer: From carcinogenesis toward therapy. Medicinal Research Reviews, 2024. **44**(4): p. 1566-1595.

Hui, K., et al., VEGFR affects miR-3200-3p-mediated regulatory T cell senescence in tumour-derived exosomes in non-small cell lung cancer. Functional & Integrative Genomics, 2024. **24**(2): p. 31.

Kazmi, S.M.H., et al., Emerging Trends in Lung Cancer Presentation at a Leading Tertiary Oncology Center and the Need for Lung Cancer Screening in Pakistan. Cureus, 2024. **16**(9).

Frontier in Medical & Health Research

ISSN: (e) 3007-1607 (p) 3007-1593

Al-Jumaili, M.H.A., et al., Comprehensive review on the Bis–heterocyclic compounds and their anticancer efficacy. Journal of Molecular Structure, 2023. **1271**: p. 133970.

Bychkov, I., et al., Regulation of VEGFR2 and AKT signaling by Musashi-2 in lung cancer. Cancers, 2023. **15**(9): p. 2529.

Evyapan, G., N.C. Senturk, and I.S. Celik, Ornidazole Inhibits the Angiogenesis and Migration Abilities of Non-small Cell Lung Cancer (NSCLC) via Downregulation of VEGFA/VEGFR2/NRP-1 and PI3K/AKT/mTOR Pathways. Cell biochemistry and biophysics, 2024. **82**(4): p. 3277-3285.

Patel, N., et al., Investigating the role of natural flavonoids in VEGFR inhibition: Molecular modelling and biological activity in A549 lung cancer cells. Journal of Molecular Structure, 2025. **1322**: p. 140392.

Ji, T., et al., Sinensetin Inhibits Angiogenesis in Lung Adenocarcinoma via the miR-374c-5p/VEGF-A/VEGFR-2/AKT Axis. Cell Biochemistry and Biophysics, 2024. **82**(3): p. 2413-2425.

Kashyap, M., et al., A critical analysis of design, binding pattern and SAR of benzo-fused heteronuclear compounds as VEGFR-2 inhibitors. Bioorganic & Medicinal Chemistry, 2024. **115**: p. 117966.

Feng, W., et al., Association of VEGFR2 polymorphisms with clinical outcomes of anti-angiogenesis therapy in cancer patients: A systematic review and meta-analysis. European Journal of Pharmacology, 2025: p. 177299.

Liu, M. and H. Li, Apatinib has anti-tumor effects and induces autophagy in lung cancer cells with high expression of VEGFR-2. Iranian Journal of Basic Medical Sciences, 2024. **27**(11): p. 1370.

Wang, S.S., et al., Rhamnazin enhanced anti-tumor efficacy of anti-PD-1 therapy for lung cancer in mice through inhibition of PD-L1 expression. The Tohoku Journal of Experimental Medicine, 2023. **260**(1): p. 63-73.

Luo, Y.-L., et al., Inhibition of LPA-LPAR1 and VEGF-VEGFR2 signaling in IPF treatment. Drug Design, Development and Therapy, 2023: p. 2679-2690.

Zhang, C., et al., Targeting VEGF/VEGFRs pathway in the antiangiogenic treatment of human cancers by traditional Chinese medicine. Integrative cancer therapies, 2018. **17**(3): p. 582-601.

Zaky, M.Y., et al., Unraveling the anticancer potential of statins: Mechanisms and clinical significance. Cancers, 2023. **15**(19): p. 4787.

Nayarisseri, A., et al., Potential inhibitors of VEGFR1, VEGFR2, and VEGFR3 developed through Deep Learning for the treatment of Cervical Cancer. Scientific Reports, 2024. **14**(1): p. 13251.

Nafie, M.S., et al., Triazole-functionalized benzofuran and benzothiophene semicarbazides as novel VEGFR-2-targeted anti-cancer agents. Bioorganic Chemistry, 2025: p. 108702.

Budipramana, K. and F. Sangande, Structural and molecular insights from dual inhibitors of EGFR and VEGFR2 as a strategy to improve the efficacy of cancer therapy. Chemical Biology & Drug Design, 2024. **103**(5): p. e14534.

Wang, X., et al., Molecular bases of VEGFR-2-mediated physiological function and pathological role. Frontiers in Cell and Developmental Biology, 2020. **8**: p. 599281.

Frontier in Medical & Health Research

ISSN: (e) 3007-1607 (p) 3007-1593

Xu, X., et al., Identification of 1, 3-thiazinan-4-one urea-based derivatives as potent FLT3/VEGFR2 dual inhibitors for the treatment of acute myeloid leukemia. Journal of Molecular Structure, 2022. **1250**: p. 131862.

Beker, H.K. and I. Yıldırım, Anticancer Activity–Structure Relationship of Quinolinone-Core Compounds: An Overall Review. Pharmaceutical Chemistry Journal, 2023. **56**(10): p. 1333-1343.

Gach-Janczak, K., et al., Quinolin-4-ones: Methods of Synthesis and Application in Medicine. Molecules, 2025. **30**(1): p. 163.

Liu, K., et al., Discovery of novel 2-(trifluoromethyl) quinolin-4-amine derivatives as potent antitumor agents with microtubule polymerization inhibitory activity. Bioorganic Chemistry, 2023. **139**: p. 106727.

Shinde, A., et al., Synthesis of 2-(6-substituted quinolin-4-yl)-1-(4-aryl-1H-1, 2, 3-triazol-1-yl) propan-2-ol as potential antifungal and antitubercular agents. European Journal of Medicinal Chemistry Reports, 2023. **7**: p. 100102.

Abd El-Lateef, H.M., et al., Novel quinolin-4-ylcarbonylhydrazine having N-(3-arylacryloyl) moiety: Design, synthesis and biological evaluation as potential cytotoxic agents against MDA-MB-231 via tubulin assembly inhibition. Journal of Molecular Structure, 2025. **1321**: p. 140214.

Shinde, A., et al., Synthesis of 2-(6-substituted quinolin-4-yl)-1-alkoxypropan-2-ol as potential antimycobacterial agents. Chemical Papers, 2023. **77**(7): p. 3791-3802.

Kilic, B. and D.S. Dogruer, Synthesis and investigation of the cholinesterase inhibitory and antioxidant capacities of some novel N'- (quinolin- 4-ylmethylene) propanehydrazides against Alzheimer's disease. Drug Development Research, 2024. **85**(3): p. e22183.

Verma, E., et al., Discovery of novel series of 4-quinolone hybrids as multi-targeting agent: Design, synthesis and H1-antihistaminic activity to treat allergic asthma. Journal of Molecular Structure, 2023. **1293**: p. 136241.

Wu, X., et al., Synthesis, structural characterization and biological activity of quinolone-based photo-induced CO release molecules as anticancer agents. Journal of Molecular Structure, 2025. **1328**: p. 141316.

Kobayashi, T., et al., Discovery of flometoquin, a novel quinoline insecticide. Journal of Pesticide Science, 2023. **48**(4): p. 168-174.

Munna, M.M.R., et al., Unveiling promising phytocompounds from Moringa oleifera as dual inhibitors of EGFR (T790M/C797S) and VEGFR-2 in non-small cell lung cancer through in silico screening, ADMET, dynamics simulation, and DFT analysis. Journal of Genetic Engineering and Biotechnology, 2024. **22**(3): p. 100406.

Mohapatra, R.K., et al., Computational investigations of three main drugs and their comparison with synthesized compounds as potent inhibitors of SARS-CoV-2 main protease (Mpro): DFT, QSAR, molecular docking, and in silico toxicity analysis. Journal of King Saud University. Science, 2020. **33**(2): p. 101315.

Frontier in Medical & Health Research

ISSN: (e) 3007-1607 (p) 3007-1593

Singh, S., et al., High-throughput virtual screening of small-molecule inhibitors targeting immune cell checkpoints to discover new immunotherapeutics for human diseases. J Molecular Diversity, 2023. **27**(2): p. 729-751.

Zaman, A., et al., Sesquiterpene Lactones as Potential Cyclin B1/CDK1 Complex Inhibitors: Sesquiterpene Lactones as Potential Cyclin B1/CDK1. J Futuristic Biotechnology, 2023: p. 19-24.

Abdelgawad, M.A., et al., Design, Synthesis, Molecular Modeling, and Anticancer Evaluation of New VEGFR-2 Inhibitors Based on the Indolin-2-One Scaffold. Pharmaceuticals (Basel), 2022. **15**(11): p. 1416.

Sobhy, M.K., et al., 3D-QSAR pharmacophore modelling, virtual screening and docking studies for lead discovery of a novel scaffold for VEGFR 2 inhibitors: Design, synthesis and biological evaluation. Bioorganic chemistry, 2019. **89**: p. 102988.

El-Gazzar, M.G., et al., Design and synthesis of novel pyridazinoquinazoline derivatives as potent VEGFR-2 inhibitors: In vitro and in vivo study. Bioorganic Chemistry, 2019. **92**: p. 103251.

Chaudhari, P.J., A.R. Nemade, and A.A. Shirkhedkar, Recent updates on potential of VEGFR-2 small-molecule inhibitors as anticancer agents. RSC advances, 2024. **14**(45): p. 33384-33417.

Morcoss, M.M., et al., Novel benzimidazole/hydrazone derivatives as promising anticancer lead compounds: design, synthesis, and molecular docking study. Journal of advanced Biomedical and Pharmaceutical Sciences, 2020. **3**(2): p. 45-52.

Reang, J., et al., Redefining the significance of quinoline containing compounds as potent VEGFR-2 inhibitors for cancer therapy. Medicinal Chemistry Research, 2024. **33**(7): p. 1079-1099.

R Bhojwani, H. and U. J Joshi, Pharmacophore and docking guided virtual screening study for discovery of type I inhibitors of VEGFR-2 kinase. J Current Computer-Aided Drug Design, 2017. **13**(3): p. 186-207.

Alsaif, N.A., et al., New quinoxaline derivatives as VEGFR-2 inhibitors with anticancer and apoptotic activity: Design, molecular modeling, and synthesis. Bioorganic Chemistry, 2021. **110**: p. 104807.

Dhawale, S.A., P.S. Dabhade, and S.N. Mokale, Discovery of new quinazoline derivatives as VEGFR-2 inhibitors: Design, synthesis, and anti-proliferative studies. Anti-Cancer Agents in Medicinal Chemistry-Anti-Cancer Agents), 2023. **23**(18): p. 2042-2055.

Shahin, M.I., et al., Design, synthesis and biological evaluation of type-II VEGFR-2 inhibitors based on quinoxaline scaffold. Bioorganic chemistry, 2014. **56**: p. 16-26